THE JOURNAL OF PHYSICAL CHEMISTRY A

 VOLUME 109, NUMBER 25, JUNE 30, 2005

ARTICLES

Vibrational Energy Relaxation Rates via the Linearized Semiclassical Approximation: Applications to Neat Diatomic Liquids and Atomic−Diatomic Liquid Mixtures

Being J. Ka, Qiang Shi, and Eitan Geva*

Department of Chemistry and the FOCUS center, University of Michigan, Ann Arbor, Michigan 48109-1055

Received: March 9, 2005; In Final Form: May 5, 2005

We report the results obtained from the application of our previously proposed linearized semiclassical method for computing vibrational energy relaxation (VER) rates (*J. Phys. Chem. A* **2003**, *107*, 9059, 9070) to neat liquid oxygen, neat liquid nitrogen, and liquid mixtures of oxygen and argon. Our calculations are based on a semiclassical approximation for the quantum-mechanical force−force correlation function, which puts it in terms of the Wigner transforms of the force and the product of the Boltzmann operator and the force. The calculation of the multidimensional Wigner integrals is made feasible by the introduction of a local harmonic approximation. A systematic analysis has been performed of the temperature and mole-fraction dependences of the VER rate constant, as well as the relative contributions of centrifugal and potential forces, and of different types of quantum effects. The results were found to be in very good quantitative agreement with experiment, and they suggest that this semiclassical approximation can capture the quantum enhancement, by many orders of magnitude, of the experimentally observed VER rate constants over the corresponding classical predictions.

I. Introduction

Vibrational energy relaxation (VER) is the process where an excited vibrational mode equilibrates by transferring its excess energy into other intramolecular and/or intermolecular degrees of freedom (DOF). VER is prevalent in many systems of fundamental, technological and biological importance, and plays a central role in determining chemical reactivity. It is therefore not surprising that the measurement and calculation of VER rates have received much attention over the past few decades.[1−46] Recent theoretical and computational studies of VER have been mostly based on the Landau−Teller formula,[15,47,48] which gives the VER rate constant in terms of the Fourier transform (FT), at the vibrational frequency, of the *quantum-mechanical* autocorrelation function of the fluctuating force exerted on the relaxing mode by the other DOF.

As was pointed out by several authors, replacing the quantum-mechanical force autocorrelation function by its classical counterpart is in general unjustified. This is because in most cases, the frequency of the relaxing vibrational mode is either comparable to or larger than $k_BT/\hbar$. Indeed, discrepancies by many orders of magnitude have been reported between experimentally measured VER rates and corresponding predictions that were based on classical molecular dynamics (MD) simulations. At the same time, the exact calculation of real-time quantum-mechanical correlation functions for general anharmonic many-body systems remains far beyond the reach of currently available computer resources, due to the exponential scaling of the computational effort with the number of DOF.[49] The most popular approach for dealing with this difficulty, in the case of VER, is based on multiplying the classical prediction for the VER rate constant by a frequency-dependent *quantum correction factor* (*QCF*).[7,50−65] In fact, a variety of different

* Corresponding author. E-mail: eitan@umich.edu.

10.1021/jp051223k CCC: $30.25
Published on Web 06/08/2005

approximate QCFs have been proposed in the literature. Unfortunately, estimates obtained from different QCFs can differ by orders of magnitude, and particularly so when high-frequency vibrations are involved. Thus, the development of more rigorous methods for computing VER rate constants is clearly highly desirable.

In two previous papers,[66,67] we have proposed a more rigorous approach for calculating VER rate constants, which is based on linearizing the forward−backward action in the path integral expression for the quantum force autocorrelation function (the linearization is with respect to the difference between the forward and backward paths[68]). It should be noted that the same approximation can be derived in several other ways, including linearization of the forward−backward action in the semiclassical initial value representation approximation for the correlation function,[69−75] and starting from the Wigner representation formalism.[76] The resulting *linearized semiclassical* (*LSC*) *approximation*, for a general real-time quantum mechanical correlation function, is given by [here, as in the rest of this paper, we use boldface symbols for vectors, and capped symbols (e.g., $\hat{A}$) for operators]:

$$\mathrm{Tr}(e^{-\beta\hat{H}}e^{i\hat{H}t/\hbar}\hat{B}e^{-i\hat{H}t/\hbar}\hat{A}) \approx \frac{1}{(2\pi\hbar)^N}\int d\mathbf{q_0}\int d\mathbf{p_0}(\hat{A}e^{-\beta\hat{H}})_W(\mathbf{q_0},\mathbf{p_0})B_W(\mathbf{q}_t^{(Cl)},\mathbf{p}_t^{(Cl)}) \quad (1)$$

where N is the number of DOF, $\mathbf{q_0} = (q_0^{(1)},..., q_0^{(N)})$ and $\mathbf{p_0} = (p_0^{(1)},..., p_0^{(N)})$ are the corresponding coordinates and momenta

$$A_W(\mathbf{q},\mathbf{p}) = \int d\mathbf{\Delta}\, e^{-i\mathbf{p}\Delta/\hbar}\langle\mathbf{q}+\mathbf{\Delta}/2|\,\hat{A}\,|\mathbf{q}-\mathbf{\Delta}/2\rangle \quad (2)$$

is the Wigner transform of the operator $\hat{A}$,[77] and $\mathbf{q}_t^{(Cl)} = \mathbf{q}_t^{(Cl)}(\mathbf{q_0},\mathbf{p_0})$ and $\mathbf{p}_t^{(Cl)} = \mathbf{p}_t^{(Cl)}(\mathbf{q_0},\mathbf{p_0})$ are propagated *classically* with the initial conditions $\mathbf{q_0}$ and $\mathbf{p_0}$. The major advantage of the LSC approximation has to do with its computational feasibility (although computing the Wigner transform in systems with many DOF is not trivial[66,67,70]). The LSC approximation has the additional attractive features of being exact at $t = 0$, at the classical limit, and for harmonic systems. Its main disadvantage has to do with the fact that it can only capture quantum dynamical effects that arise from short-time interferences between the various trajectories (the longer time dynamics is purely classical).[71] However, it should be noted that in condensed phase systems in general, and in the case of high-frequency VER in particular, the quantities of interest are often dominated by the short-time dynamics of the correlation functions.

In practice, using the LSC approximation, eq 1, requires the calculation of the phase-space integrals underlying the Wigner transforms. The numerical calculation of those integrals is extremely difficult in the case of many-body anharmonic systems, because of the oscillatory phase factor, $e^{-i\mathbf{p}_0\Delta/\hbar}$, in the integrand. In refs 66 and 67, this problem was dealt with by using a local harmonic approximation (LHA), which allowed for an analytical evaluation of the Wigner integral. The emerging LHA−LSC approximation has been tested on several benchmark problems in ref 66, and it was found to be in very good agreement with the exact results or their best estimates. It was also observed that high frequency VER is dominated by a purely quantum mechanical term which is not accounted for in classical MD simulations. The first application of the LHA−LSC method to a molecular liquid was reported in ref 67, where it was used for calculating the extremely slow ($k_{0\leftarrow1} = 395\ s^{-1}$) and highly quantum-mechanical ($\hbar\omega/k_BT = 29$) VER rate constant in neat liquid oxygen at 77 K. The VER rate constant obtained via the LHA−LSC approximation was found to be 4 orders of magnitude larger than the corresponding classical prediction, and in very good quantitative agreement with experiment.

In this paper, we present a detailed analysis of VER rates, as obtained via the LHA−LSC approximation, in neat diatomic liquids and diatomic-atomic liquid mixtures. The following aspects, that were not discussed in previous papers, are considered: (1) the temperature dependence of the VER rate constant (in the case of neat liquid oxygen); (2) the mole fraction dependence (in the case of argon−oxygen liquid mixtures); (3) the relative importance of different quantum effects; (4) the relative contributions of centrifugal and potential forces. In addition, we also report the results obtained via the LHA−LSC approximation for the VER rate constant in liquid nitrogen at 77 K. A comparison to the experimental results and the corresponding predictions obtained by using QCFs is also provided.

The structure of the remainder of this paper is as follows. The model Hamiltonian of a liquid atomic−diatomic mixture and theoretical framework for VER calculations are outlined in section II. An overview of our LHA−LSC method for calculating VER rates is given in section III. The simulation techniques used for calculating the LHA−LSC approximation for the force autocorrelation functions are described in section IV. The results for VER in neat liquid oxygen, neat liquid nitrogen and argon−oxygen liquid mixtures are reported and analyzed in section V. We conclude in section VI with a summary of the main results and some discussion on their significance. Explicit mathematical expressions for quantities required for the evaluation of the LHA−LSC approximation are provided in the Appendix.

II. Model

The atomic−diatomic liquid mixture model that we used has been adopted from ref 78, where it was used for calculating VER rate constants within the framework of the QCF approach. We consider a liquid mixture that consists of N_a atoms and $N_m + 1$ diatomic molecules, where one of the molecules is vibrationally excited, while the rest are assumed to be rigid (the case of $N_a = 0$ corresponds to a neat diatomic liquid). The overall Hamiltonian is given by

$$\hat{H} = \hat{H}_q + \hat{H}_b - \hat{q}\hat{F} \quad (3)$$

where

$$\hat{H}_q = \frac{\hat{p}^2}{2\mu} + \frac{1}{2}\mu\omega^2\hat{q}^2 \quad (4)$$

is the intramolecular vibrational Hamiltonian of the relaxing diatomic molecule ($\hat{q}$, $\hat{p}$, μ and ω are the corresponding coordinate, momentum, reduced mass, and frequency, respectively);

$$\hat{H}_b = \sum_{j=1}^{N_a}\frac{(\hat{P}_a^{(j)})^2}{2M_a} + \sum_{j=0}^{N_m}\left(\frac{(\hat{P}_m^{(j)})^2}{2M_m} + \frac{(\hat{L}^{(j)})^2}{2I}\right) + \sum_{j=0}^{N_m-1}\sum_{k=j+1}^{N_m}\sum_{\alpha,\beta=1}^{2}\phi_{mm}(|\hat{\mathbf{r}}^{(j\alpha)} - \hat{\mathbf{r}}^{(k\beta)}|) + \sum_{j=1}^{N_a-1}\sum_{k=j+1}^{N_a}\phi_{aa}(|\hat{\mathbf{r}}^{(j)} - \hat{\mathbf{r}}^{(k)}|) + \sum_{j=1}^{N_a}\sum_{k=0}^{N_m}\sum_{\alpha=1}^{2}\phi_{am}(|\hat{\mathbf{r}}^{(j)} - \hat{\mathbf{r}}^{(k\alpha)}|) \quad (5)$$

is the overall Hamiltonian of the translational and rotational DOF [M_a is the atomic mass, M_m is the molecular mass, I is the moment of inertia of the diatomic molecule, $\hat{P}_a^{(j)}$ is the momentum of the jth atom, $\hat{P}_m^{(j)}$ is the center of mass momentum of the jth diatomic molecule, $\hat{L}^{(j)}$ is the angular momentum of the jth diatomic molecule, $\hat{\mathbf{r}}^{(k)}$ is the position of the jth atom, and $\hat{\mathbf{r}}^{(j\alpha)}$ is the position of the α site on the jth diatomic molecule ($\alpha = 1, 2$)]; $-\hat{q}\hat{F}$ is the coupling between the relaxing vibrational mode and the other DOF.

The main quantity of interest is $\hat{F}$, which corresponds to the force exerted on the vibrational mode of the relaxing molecule by the translational and rotational DOF. This force consists of a sum of potential[79−81] and centrifugal[82,83] terms ($\hat{F}_U$ and $\hat{F}_T$, respectively). Identifying the zeroth molecule as the relaxing molecule, those terms are explicitly given by

$$\hat{F}_U = \frac{1}{2}\sum_{j=1}^{N_m}\sum_{\alpha,\beta=1}^{2}\phi'_{mm}(|\hat{\mathbf{r}}^{(j\alpha)} - \hat{\mathbf{r}}^{(0\beta)}|)\frac{(\hat{\mathbf{r}}^{(j\alpha)} - \hat{\mathbf{r}}^{(0\beta)})\cdot\hat{\mathbf{u}}^{(0\beta)}}{|\hat{\mathbf{r}}^{(j\alpha)} - \hat{\mathbf{r}}^{(0\beta)}|} + \frac{1}{2}\sum_{j=1}^{N_a}\sum_{\beta}\phi'_{am}(|\hat{\mathbf{r}}^{(j)} - \hat{\mathbf{r}}^{(0\beta)}|)\frac{(\hat{\mathbf{r}}^{(j)} - \hat{\mathbf{r}}^{(0\beta)})\cdot\hat{\mathbf{u}}^{(0\beta)}}{|\hat{\mathbf{r}}^{(j)} - \hat{\mathbf{r}}^{(0\beta)}|} \quad (6)$$

where $\hat{\mathbf{u}}^{(0\beta)}$ corresponds to a unit vector pointing from the center of mass of the relaxing molecule to its site β, and

$$\hat{F}_T = \frac{(\hat{L}^{(0)})^2}{Ir_e} \quad (7)$$

where r_e is the equilibrium bond length of the diatomic molecule.

The term $\hat{H}_b$ in eq 5 involves three types of pair potentials: (1) atom−atom interaction potential, $\phi_{aa}(r)$; (2) diatom−diatom site−site interaction potential, $\phi_{mm}(r)$; and (3) atom−diatom interaction potential $\phi_{am}(r)$. Following ref 78, we assume that all of those pair potentials are of the Lennard-Jones (LJ) type:

$$\phi_{ij}(r) = 4\epsilon_{ij}\left[\left(\frac{\sigma_{ij}}{r}\right)^{12} - \left(\frac{\sigma_{ij}}{r}\right)^{6}\right] \quad (8)$$

The following parameters were employed in the case of liquid mixtures of oxygen and argon: $r_e = 1.208$ Å, $\epsilon_{mm} = 48.0k_B$ K, $\sigma_{mm} = 3.0060$ Å, $\epsilon_{am} = 75.8k_B$ K, $\sigma_{am} = 3.2325$ Å, $\epsilon_{aa} = 119.8k_B$ K, $\sigma_{aa} = 3.4050$ Å. It should be noted that the values of ϵ_{mm} and σ_{mm} were adopted from ref 84, and they are different then those originally used in ref 78. It should also be noted that for the pair potential employed, the two sites coincide with the equilibrium locations of the oxygen nuclei (which is not the case for the potential used in ref 78). In the case of neat liquid nitrogen, we have employed the same values of the parameters as used in ref 57, namely $r_e = 1.094$ Å, $\epsilon_{mm} = 37.3k_B$ K, and $\sigma_{mm} = 3.310$ Å. The values of the mole fractions, temperatures, and densities used in the simulations are shown in Table 1.

TABLE 1: Values of the Mole Fractions, Temperatures and Densities Used in the Simulations

system	mole fraction	temp (K)	density (nm^{-3})	ref
neat N_2	1.0	77	17.37	90
neat O_2	1.0	60	24.13	91
	1.0	65	23.71	91
	1.0	70	23.28	91
	1.0	77	22.64	91
	1.0	80	22.41	91
	1.0	85	21.96	91
	1.0	90	21.50	91
O_2/Ar	0.30	77	22.15	78
	0.50	77	22.29	78
	0.70	77	22.43	78
	0.85	77	22.50	78

III. The Linearized Semiclassical Approximation

In this study, we focus on the relaxation from the first excited vibrational state to the ground state of a homonuclear diatomic molecule. We will also assume that the rate constant for this process is given by the Landau−Teller formula[15,47] (the assumptions underlying this expression have been discussed by many authors; e.g., see the discussion in ref 85):

$$k_{0\leftarrow 1} = \frac{1}{2\mu\hbar\omega}\tilde{C}(\omega) \quad (9)$$

where

$$\tilde{C}(\omega) = \int_{-\infty}^{\infty} dt\, e^{i\omega t}C(t) = \frac{4}{1+e^{-\beta\hbar\omega}}\int_0^{\infty} dt\, \cos(\omega t)C_R(t) = -\frac{4}{1-e^{-\beta\hbar\omega}}\int_0^{\infty} dt\, \sin(\omega t)C_I(t) \quad (10)$$

and

$$C(t) = C_R(t) + iC_I(t) = \langle\delta\hat{F}(t)\delta\hat{F}\rangle = \frac{1}{Z_b}\mathrm{Tr}[e^{-\beta\hat{H}_b}e^{i\hat{H}_b t/\hbar}\delta\hat{F}e^{-i\hat{H}_b t/\hbar}\delta\hat{F}] \quad (11)$$

is the quantum-mechanical force−force correlation function (FFCF). Here, $\langle\hat{A}\rangle = \mathrm{Tr}[e^{-\beta\hat{H}_b}\hat{A}]/Z_b$, $Z_b = \mathrm{Tr}[e^{-\beta\hat{H}_b}]$ and $\delta\hat{F} = \hat{F} - \langle\hat{F}\rangle$. Equation 9 gives the VER rate constant, $k_{0\leftarrow 1}$, in terms of the FT, at the vibrational frequency, ω, of the FFCF, $C(t)$. It should be noted that $C_R(t)$ and $C_I(t)$ in eq 10 are the real and imaginary parts of the FFCF, respectively.

The LSC approximation of the quantum-mechanical FFCF, eq 11, assumes the following form:[66−68]

$$C(t) \approx \frac{1}{Z_b}\frac{1}{(2\pi\hbar)^N}\int d\mathbf{Q_0}\int d\mathbf{P_0}\,[\delta\hat{F}e^{-\beta\hat{H}_b}]_W(\mathbf{Q_0},\mathbf{P_0})\,\delta F_W(\mathbf{q}_t^{(Cl)},\mathbf{P}_t^{(Cl)}) \quad (12)$$

Here, $\mathbf{Q}_t^{(Cl)} = \mathbf{Q}_t^{(Cl)}(\mathbf{Q_0},\mathbf{P_0})$ and $\mathbf{P}_t^{(Cl)} = \mathbf{P}_t^{(Cl)}(\mathbf{Q_0},\mathbf{P_0})$ correspond to the Cartesian coordinates and momenta of all the atoms, which are propagated classically with the initial conditions $\mathbf{Q_0}$ and $\mathbf{P_0}$. A direct calculation of this approximation in the case of an anharmonic many-body system, would require the calculation of the multidimensional Wigner phase-space integral in eq 2. Unfortunately, it is extremely difficult to perform this calculation via conventional Monte Carlo (MC) techniques, due to the oscillatory phase factor, $e^{-i\mathbf{P}_0\Delta/\hbar}$, in the integrand. This problem can be circumvented by employing a local harmonic approximation (LHA), whereby one effectively expands $\hat{H}_b$ to second order around $\mathbf{Q_0}$, followed by an analytical integration of the resulting Gaussian integral over Δ. The resulting LHA−LSC approximation for the FFCF assumes the following form:

$$C(t) \approx \int d\mathbf{Q_0}\frac{\langle\mathbf{Q_0}|e^{-\beta\hat{H}_b}|\mathbf{Q_0}\rangle}{Z_b}\int d\mathbf{P}_{n,0}\prod_{j=1}^{N}\left(\frac{1}{\alpha^{(j)}\pi\hbar^2}\right)^{1/2}\exp\left[-\frac{(P_{n,0}^{(j)})^2}{\hbar^2\alpha^{(j)}}\right][\delta F_U(\mathbf{Q_0}) + \delta F_T(\mathbf{P}_{n,0}) + D_U(\mathbf{Q_0},\mathbf{P}_{n,0}) + D_T(\mathbf{Q_0},\mathbf{P}_{n,0})][\delta F_U(\mathbf{Q}_t^{(Cl)}) + \delta F_T(\mathbf{P}_{n,t}^{(Cl)})] \quad (13)$$

Here, $\{\hat{P}_n^{(k)}\}$ are mass-wighted normal mode momenta, as obtained from the expansion of $\hat{H}_b$ to second order around $\mathbf{Q_0}$ (the LHA), and $\alpha^{(j)} = \Omega^{(j)} \coth[\beta\hbar\Omega^{(j)}/2]/\hbar$, where $\{(\Omega^{(k)})^2\}$ are the eigenvalues of the corresponding Hessian matrix (explicit expressions of the potential derivatives underlying the LHA for the model considered here are provided in the appendix). The terms $D_T(\mathbf{Q_0},\mathbf{P}_{n,0})$ and $D_U(\mathbf{Q_0},\mathbf{P}_{n,0})$, which originate from the centrifugal and potential forces, respectively, are purely quantum-mechanical [i.e., they vanish at the classical ($\hbar \rightarrow 0$) limit]. Those terms represent quantum nonlocality, and can be traced back to the fact that $[\hat{F}e^{-\beta\hat{H}_b}]_w \neq [\hat{F}]_w \times [e^{-\beta\hat{H}_b}]_w$. Explicit expressions for those terms can be found in ref 67, and some detailed expressions of quantities required for their evaluation (for the model under discussion) are provided in the Appendix. Another quantum-mechanical effect is introduced by the fact that the initial sampling of the positions and momenta is nonclassical. More specifically, the initial sampling of the positions is based on the exact quantum mechanical position probability density, $\langle\mathbf{Q_0}|e^{-\beta\hat{H}_b}|\mathbf{Q_0}\rangle/Z_b$, while the initial sampling of the momenta is based on the nonclassical probability density $\prod_{j=1}^{N} (1/\alpha^{(j)}\pi\hbar^2)^{1/2} \exp[-(P_{n,0}^{(j)})^2/\hbar^2\alpha^{(j)}]$.

IV. Simulation Techniques

The computational algorithm employed for calculating the approximate FFCF in eq 13 is similar to that described in refs 66 and 67 and follows the following steps.

1. In the first step, we sample the initial positions of all the atoms in the simulation cell via a PIMD simulation, based on the probability density $\text{Prob}(\mathbf{Q_0}) = \langle\mathbf{Q_0}|e^{-\beta\hat{H}_b}|\mathbf{Q_0}\rangle/Z_b$. It should be noted that the initial configurations sampled must also satisfy the constraints imposed by the rigidity of the molecules.[67] We performed such PIMD simulations with an overall number of 500 atoms *and* molecules in the simulation cell. Each atom (either belonging to a molecule or not) was represented by a chain polymer consisting of 16 beads. Thermalization was imposed by attaching a Nose-Hoover chain thermostat to each of the beads, and the dynamics has been computed by using the velocity Verlet algorithm.[86] The sampling was performed by choosing random beads from snapshots of the isomorphic liquid of cyclic polymers.

2. In the second step, we randomly select one of the molecules in the simulation cell and designate it as the relaxing molecule. Next, the 20−30 atoms and molecules which are closest to the relaxing molecule are identified, and form the "active cluster".[67] The next 60−80 closest atoms and molecules are then identified, and their positions are kept fixed throughout the rest of the simulation (those frozen atoms and molecules serve as a static cage which prevents the cluster from falling apart).

3. In the third step, we calculate the normal-mode frequencies and transformation matrix for the atoms in the active cluster, via the Jacobi method,[87] and use them in order to sample the initial normal mode momenta. Here too, we restrict ourselves to normal-mode displacements which satisfy the constraints imposed by the rigidity of the molecules.[67]

4. In the fourth step, the cluster atoms and molecules are allowed to evolve in time via a classical MD simulation (still maintaining the constraints imposed by the rigidity of the molecules[67]), to obtain the force on the relaxing molecule at time *t*. The velocity Verlet algorithm with a time step of 4 fs has been used in the simulations reported here.

5. Steps 1−4 are repeated for many initial cluster-cage configurations, and the results are averaged in order to obtain the desired FFCF. The results reported below are based on averaging $(1-4) \times 10^6$ initial cluster-cage configurations.

TABLE 2: $k_{0\leftarrow1}/s^{-1}$ for Neat Liquid O_2 and Neat Liquid N_2 at 77 K

	O_2	N_2
experiment[1,6]	395 ± 18	$(1.8 \pm 0.5) \times 10^{-2}$
classical	$(285 \pm 31) \times 10^{-4}$	$(3.1 \pm 0.4) \times 10^{-10}$
LHA-LSC	783 ± 62	$(1.9 \pm 0.3) \times 10^{-3}$
harmonic	8.3 ± 0.4	$(9.8 \pm 1.0) \times 10^{-7}$
Egelstaff	1373 ± 113	$(3.6 \pm 0.7) \times 10^{-3}$
mixed harmonic-Schofield	677 ± 27	$(1.4 \pm 0.2) \times 10^{-3}$

Once the FFCF is obtained, its FT is calculated. All of the results reported below were based on the cosine transform of the real part of the FFCF [see eq 10]. The FT of the FFCF at the very high vibrational frequencies of diatomic molecules like oxygen (1553 cm^{-1}) and nitrogen (2327 cm^{-1}) is a very small number, and therefore very difficult to compute directly. Following the common practice, we instead extrapolate the exponential gap law, which usually emerges at low frequencies, to much higher frequencies.[88,89] Assuming that this extrapolation is the major source of error, we evaluated the error bars reported for the VER rate constants based on the least-squares fit to the corresponding linear frequency dependence of the VER rate constant (on a semilog scale).

V. Results

We start out with a detailed analysis of VER in neat liquid oxygen and neat liquid nitrogen, at 77 K. The results obtained for the VER rate constant via the LHA−LSC method are presented in Table 2, alongside the experimental results[1,6] and predictions based on the best performing QCFs (cf. ref 66 for the explicit definitions of those QCFs). It should be noted that the results for oxygen are slightly different then those reported in our previous paper.[67] The difference between the results is mostly due to more extensive averaging and the somewhat more refined extrapolation procedure employed in the present paper. As can be seen, the LHA−LSC-based prediction for the VER rate constant in neat liquid oxygen is larger by a factor of about two than the experimental result. This represents a dramatic improvement in comparison to the classical prediction which is smaller than the experimental result by a factor of about 10^4. It should also be noted that the Egelstaff and mixed harmonic−Schofield QCFs happen to yield predictions of similar quality to the one based on LHA−LSC.

In the case of neat liquid nitrogen, the classical prediction for the VER rate constant is smaller by a factor of 10^8 in comparison to the experimental value. This can be attributed to the significantly higher vibrational frequency of nitrogen. At the same time, the LHA−LSC-based prediction for the VER rate constant turns out to be smaller only by a factor of 10 in comparison to the experimental value. In fact, it has been argued that the rate of nonradiative VER in neat liquid nitrogen is so slow, such that the experimentally measured value is actually dominated by radiative VER.[1,57] If so, the nonradiative VER rate constant should in fact be smaller than the experimental value. The LHA−LSC-based prediction is consistent with this point of view, as well as with the reported estimated upper bound for the nonradiative VER rate constant (0.004 s^{-1}).[1] Finally, here too, one observes that the Egelstaff and mixed harmonic−Schofield QCFs yield predictions which happen to be of similar quality to LHA−LSC.

In Figures 1 and 2, we show the FFCF in the time and frequency domains (the latter is shown on a semilog plot), as obtained via the LHA−LSC method, for neat liquid oxygen and neat liquid nitrogen at 77 K. Figures 1a and 2a also show the contributions to the FFCF from the classical $[F_U + F_T][F_U(t)$

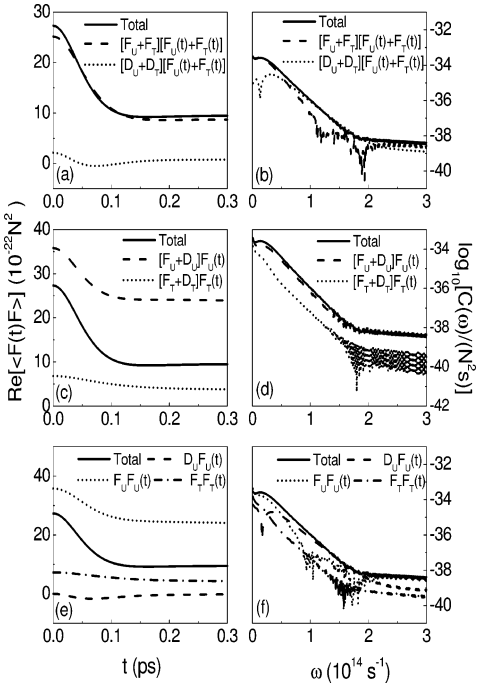

Figure 1. Force−force correlation function (a, c, e) and its Fourier transform (b, d, f), for neat liquid oxygen at 77 K. Also shown are the relative contributions of the classical-like and quantum nonlocal terms (a, b), the centrifugal and potential forces (c, d), and a partial breakup of the potential and centrifugal terms into classical and nonclassical terms (e, f).

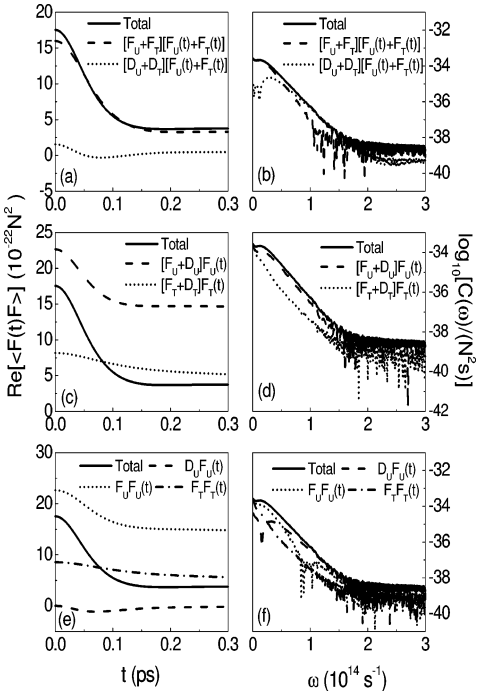

Figure 2. Same as Figure 1, for neat liquid nitrogen at 77 K.

$+ F_T(t)]$ term and nonclassical $[D_U + D_T][F_U(t) + F_T(t)]$ term (the initial sampling is nonclassical in both cases). The contributions of those two terms to the FT of the FFCF are shown in Figures 1b and 2b. While the classical term is observed to dominate the FFCF in the time domain, the nonclassical term is observed to dominate the behavior of its FT, and therefore VER, at high frequencies. It is important to note that the nonclassical term vanishes at the classical limit, and can therefore not be directly accounted for by classical MD simulations. Furthermore, there seems to be no straightforward way of representing the contribution of this nonclassical term in the form of some sort of a multiplicative QCF.

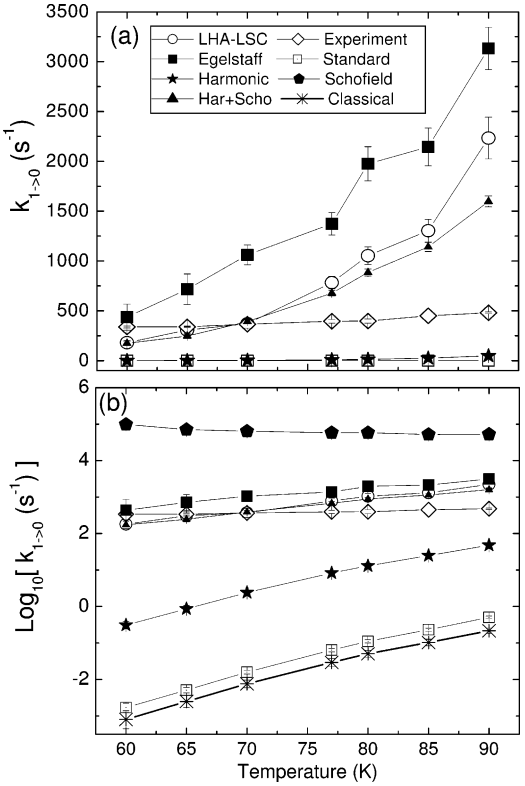

Figure 3. Temperature dependence of the VER rate constant in neat liquid oxygen on regular (upper panel) and semilog (lower panel) scales. Shown are the results obtained via the LHA−LSC method, as well as the corresponding experimental rate constants, and results obtained by using a variety of QCFs.

Figures 1c and 2c show the contributions to the FFCF from the terms, $[F_T + D_T]F_T(t)$ and $[F_U + D_U]F_U(t)$], which arise from the centrifugal and potential forces, respectively (cross terms are not shown explicitly, but can be deduced from the difference between the overall FFCF and the diagonal contributions). The corresponding contributions in the frequency domain are shown in Figures 1d and 2d. The VER rate is clearly dominated by the potential force in both time and frequency domains, and particularly so at high frequencies. This observation is reminiscent of similar observations made based on classical simulations. However, a closer inspection reveals that the main contribution to the FT at high frequencies comes from the nonclassical potential force term, $D_UF_U(t)$. Furthermore, the contribution, at high frequencies, of the classical-like potential term, $F_UF_U(t)$, appears to be comparable to, and even smaller than, that of the classical-like centrifugal term, $F_TF_T(t)$ [see Figures 1e,f and 2e,f]. This behavior, which is clearly different from that observed in classical simulations, can be attributed to the nonclassical sampling.

We next consider the dependence of the VER rate on temperature. To this end, we calculated the VER rate constant for neat liquid oxygen at seven different temperatures between 60 and 90 K. Our choice of system and temperature range was motivated by the availability of experimental results, which one can compare to in the lack of numerically exact benchmark calculations.[6] The results obtained via LHA−LSC are shown on regular and semilog plots in Figure 3, alongside the experimental values[6] and predictions obtained by using various QCFs. Similarly to the experimental results, the LHA−LSC-based VER rate constant is seen to monotonically increase with

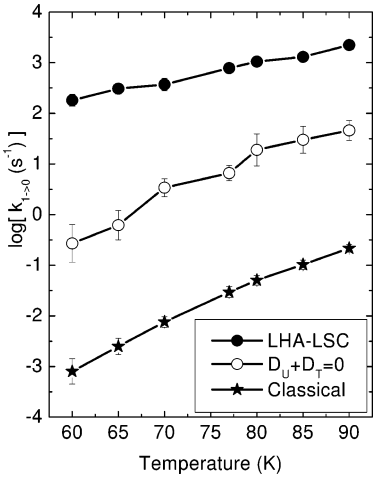

Figure 4. Relative contributions of nonclassical sampling and quantum nonlocal terms, in the case of neat liquid oxygen. Shown are the VER rate constants obtained at different temperatures, by using nonclassical initial sampling and neglecting contributions from the nonlocal terms, D_U and D_T (white circles). Also shown, for the sake of comparison, are the LHA−LSC results (black circles) and classical results, i.e., with classical sampling and neglecting the nonlocal terms (stars).

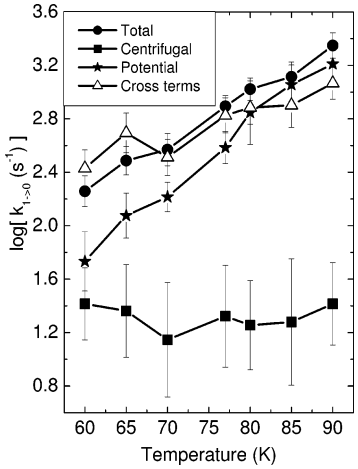

Figure 5. Relative contributions of centrifugal and potential forces, in the case of neat liquid oxygen. Shown are the VER rate constants obtained via LHA−LSC, at different temperatures, by taking into account contributions from either only the centrifugal force, (squares), or potential force (stars), or the cross terms (triangles). The overall VER rate constants are also shown, for the sake of comparison (circles).

temperature. Classical mechanics, as well as most QCFs, also predict VER rate constants that monotonically increase with temperature (the only exception is the Schofield QCF, where the VER rate constant is a monotonically decreasing function of temperature). The quantitative agreement between LHA−LSC and the experimental results remains very good throughout the entire temperature range. The results obtained via the LHA−LSC method are also seen to be rather similar to predictions based on the Egelstaff and mixed harmonic−Schofield QCFs. Interestingly, when compared on a regular scale, LHA−LSC seem to predict a temperature dependence which is significantly stronger in comparison to experiment (as do the Egelstaff and mixed harmonic−Schofield QCFs). The specific origin for this discrepancy is hard to trace, but could be conceivably due to inaccuracies in the interaction potentials.

We have also explored the relative importance of nonclassical initial sampling as a function of temperature. To this end, we have recalculated the VER rate constants for neat liquid oxygen within the temperature range (60, 90 K), without the contributions from the nonlocal quantum terms, D_U and D_T (cf. Figure 4). As the results clearly demonstrate, nonclassical initial sampling alone cannot quantitatively account for the enhancement of the VER rate relative to the corresponding classical result. More specifically, while the LHA−LSC VER rate constant is about 4 orders of magnitude larger than the classical result, nonclassical sampling can only account for an enhancement by 2 orders of magnitude. To obtain a quantitative agreement with experiment, it is necessary to include the nonlocal terms D_U and D_T. We have also attempted a calculation of the VER rate which included the nonlocal terms, but was based on *classical* sampling. We have found that such a treatment does not give rise to an exponential gap law at intermediate frequencies. Thus, in this case, it was not possible to obtain meaningful results by performing an extrapolation to higher frequencies.

Another interesting aspect of VER in diatomic liquids has to do with the relative contributions of potential and centrifugal forces. To this end, we recalculated the VER rate constant in liquid oxygen by only taking into account either the potential force, the centrifugal force, or the cross terms. The results are presented in Figure 5. It should be noted that the centrifugal contribution is characterized by relatively large error bars, which is indicative of deviations from an exponential gap law (i.e., linearity as a function of frequency on a semilog plot). One observation that can be made based on Figure 5, is that the potential and cross terms dominate VER within the temperature range considered. However, it should be noted that the contributions from the potential and cross terms decrease rapidly with temperature, while the contribution of the centrifugal term is rather insensitive to temperature. This observation is qualitatively different from the corresponding classical result, where the centrifugal term is seen to rapidly decrease with decreasing temperature. Further analysis seems to suggest that this insensitivity originates from nonclassical momentum sampling. In this context, it is interesting to note that the width of the momentum sampling function becomes insensitive to temperature at lower temperatures and higher frequencies [cf. eq 13], and note that $\alpha^{(j)} \rightarrow \Omega^{(j)}/\hbar$ when $\beta\hbar\Omega^{(j)} \gg 1$. Exploring whether the centrifugal term becomes the dominant one at even lower temperatures is not possible since oxygen freezes at 54.8 K.

We next consider the dependence of the VER rate constant on the oxygen mole fraction, in oxygen−argon liquid mixtures, at 77 K. Here, too, the choice of system is motivated by the availability of experimentally measured VER rate constants.[6] The LHA−LSC results are presented in Figure 6, in terms of the ratio $k_{0\leftarrow1}(x)/k_{0\leftarrow1}(1)$, where $k_{0\leftarrow1}(x)$ is the actual VER rate constant for a mixture where the oxygen mole fraction is x. Also shown are the corresponding experimental results, and predictions based on classical mechanics and the Egelstaff QCF. It should be noted that the other QCFs correspond to multiplying the classical VER rate constant by a factor, which is independent of x, and therefore gives the same values of $k_{0\leftarrow1}(x)/k_{0\leftarrow1}(1)$ as classical mechanics. The VER rate is seen to nonlinearly increase with increasing oxygen mole fraction, and the results obtained via all methods indeed follow this trend. The LHA−LSC results are also seen to be in very good quantitative agreement with the experimental results, except at the lowest values of the oxygen mole fraction. While the agreement between the experimental results and classical predictions (as well as the predictions of all QCFs, except for Egelstaff) is reasonable, it is clearly not as good as the agreement with the LHA−LSC results. The predictions based on the Egelstaff QCF lie between the classical and LHA−LSC predictions. It should

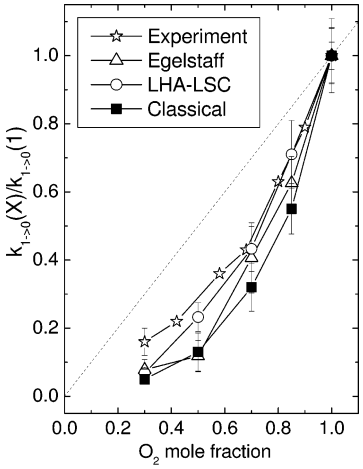

Figure 6. Oxygen mole-fraction dependence of VER rates in liquid mixtures of argon and oxygen, at 77 K. Shown are the results obtained via the LHA−LSC approximation (circles), as well as the corresponding experimental values (stars), and predictions based on classical mechanics (squares) and the Egelstaff QCF (triangles).

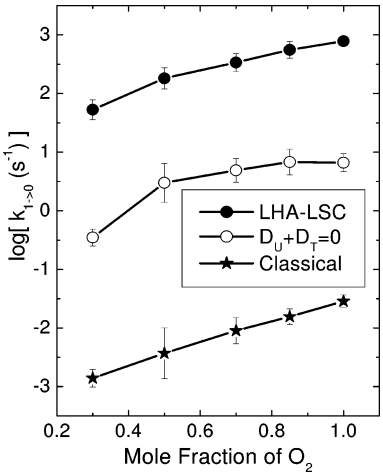

Figure 7. Relative contributions of nonclassical sampling and nonlocal terms in liquid mixtures of oxygen and argon. Shown are the VER rate constants obtained at different oxygen mole fractions, by using nonclassical initial sampling and neglecting contributions from the nonlocal terms, D_U and D_T (white circles). Also shown, for the sake of comparison, are the LHA−LSC results (black circles) and classical results, i.e., with classical sampling and neglecting the quantum nonlocal terms (stars).

be noted that Everitt and Skinner[78] have previously reported a better agreement between experiment and predictions based on the Egelstaff QCF. However, this result was based on an older version of the oxygen−oxygen pair potential and a different extrapolation procedure. As it turns out, the agreement between the Egelstaff QCF and experiment becomes slightly worse when one employs a presumably improved pair potential developed in a later paper by the same authors[84] and our extrapolation procedure (it should be noted that a technical inconsistency does not allow for using the ansatz-based procedure employed in ref 78 in the case of the new pair potential).

Finally, we consider the relative importance of nonclassical sampling, and of potential vs centrifugal forces, as a function of mole fraction. The corresponding results are displayed in Figures 7 and 8. As in the case of neat liquids, we found that nonclassical sampling alone cannot capture the quantum mechanical enhancement of the VER rate to its fullest extent, and that including the quantum nonlocal terms is essential for obtaining a quantitative agreement with experiment. This

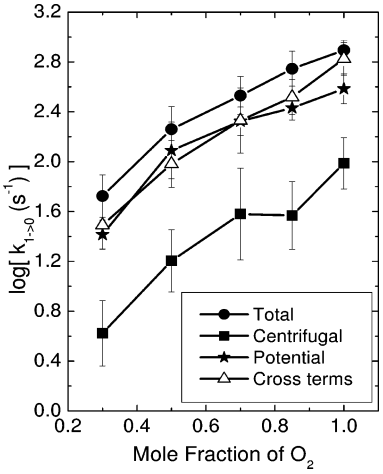

Figure 8. Relative contributions of centrifugal and potential forces, in liquid mixtures of oxygen and argon. Shown are the VER rate constants obtained via LHA−LSC, at different mole fractions, by taking into account contributions from either only the centrifugal force, (squares), potential force (stars), or the cross terms (triangles). The overall VER rate constants are also shown, for the sake of comparison (circles).

observation is also seen to be rather insensitive to the mole fraction [cf. Figure 7]. The results displayed in Figure 8 show that the contributions from the potential, centrifugal and cross terms increase with increasing oxygen mole fraction. Since the potential contribution dominates VER at the temperature considered (77 K), it appears that the overall increase of the VER rate with increasing oxygen mole fraction can be primarily attributed to an increase in the number of intermolecular vibration−rotation relaxation pathways.

VI. Summary

Within the framework of the Landau−Teller formalism, VER rates are dictated by the high frequency FT of the quantum-mechanical FFCF. The latter is typically dominated by the short time dynamics of the FFCF, which the LSC approximation appears to be able to capture accurately. In previous papers, we have demonstrated the accuracy and feasibility of the LHA−LSC methodology in the case of several benchmark problems[66] and for neat liquid oxygen at 77 K.[67] In the present paper, we have extended the testing to other systems (neat liquid nitrogen and liquid mixtures of argon and oxygen). We have also provided a systematic analysis of the roles of nonclassical sampling vs nonlocal terms and potential vs centrifugal terms, as well as their dependence on temperature and the mixture consistency. The predictions obtained via the LHA−LSC method were found to be in very good agreement with experiment in all of the cases considered, thereby demonstrating its feasibility, flexibility and accuracy. The analysis also sheds new light on the quantum nature of VER. More specifically, nonclassical sampling alone is unable to quantitatively account for the enhancement of the quantum mechanical VER rate relative to its classical counterpart. However, quantitative predictions can be obtained by accounting for the quantum nonlocal terms. Furthermore, whereas VER is seen to be dominated by the potential force, it is the nonclassical potential force term which is responsible for it. The contributions of the classical-like potential and centrifugal terms are observed to be negligible in comparison to this term, and turn out to be comparable in size because of the nonclassical initial sampling.

The results of the present paper further establish the LHA−LSC method as an attractive alternative to the commonly used

approach, which is based on the use of QCFs. Applications to polyatomic molecular liquids, as well as the development of more efficient computational tools, are currently underway in our group and will be reported in future publications.

Acknowledgment. The authors are grateful for financial support from the National Science Foundation through Grant No. CHE-0306695.

Appendix: Useful Expressions for Calculating the LHA−LSC Approximation of the FFCF

In this appendix, we provide explicit expressions of quantities which are required for calculating the LHA−LSC approximation of the FFCF in eq 13. The treatment is specialized to the case of a liquid mixture which constitutes of atoms and homonuclear diatomic molecules (cf. section II). The following notations and conventions are used throughout:

1. N_{act} is the number of atoms and molecules in the active cluster, while N_t is the overall number of atoms and molecules in the active cluster and frozen cage. The atoms and molecules are indexed such that $i = 0, ..., N_{act} - 1$ correspond to the atoms and molecules in the active cluster, ordered by their distance from the tagged molecule ($i = 0$ corresponds to the tagged molecule), while $i = N_{act}, ..., N_{t-1}$ correspond to the atoms and molecules that constitute the frozen cage.

2. Atoms are treated as single-site molecules. The variable $n_s(i)$ indicates the number of sites, such that $n_s(i) = 1$ if the index i corresponds to an atom, while $n_s(i) = 2$ if the index i corresponds to a molecule.

3. $\mathbf{r}^{i\alpha,j\beta} = \mathbf{r}^{(i\alpha)} - \mathbf{r}^{(j\beta)}$ is the vector that points from site β on the jth atom/molecule to site α on the ith atom/molecule. $x^{i\alpha,j\beta}$, $y^{i\alpha,j\beta}$ and $z^{i\alpha,j\beta}$ correspond to the x, y, and z coordinates of this vector. $r^{i\alpha,j\beta} = |\mathbf{r}^{i\alpha,j\beta}|$ corresponds to the distance between those sites.

4. $\phi(r^{i\alpha,j\beta})$ corresponds to $\phi_{aa}(r^{i\alpha,j\beta})$ or $\phi_{am}(r^{i\alpha,j\beta})$ or $\phi_{mm}(r^{i\alpha,j\beta})$, depending on whether the sites $\mathbf{r}^{i\alpha}$ and $\mathbf{r}^{j\beta}$ belong to an atom or a molecule.

5. $\mathbf{r} = \mathbf{r}^{(i\alpha,\mathbf{0}\beta)}$ corresponds to the vector pointing from the β site of the tagged molecule to the α site on the ith atom/molecule. $x = x^{(i\alpha,0\beta)}$, $y = y^{(i\alpha,0\beta)}$ and $z = z^{(i\alpha,0\beta)}$ correspond to the x, y, and z coordinates of this vector, and $r = |\mathbf{r}|$ corresponds to its length.

6. $\bar{\alpha} = 3 - \alpha$ ($\bar{\beta} = 3 - \beta$), such that if $\alpha = 1$, then $\bar{\alpha} = 2$ and vice versa.

7. $\bar{\mathbf{r}} = \mathbf{r}^{(i\alpha,\mathbf{0}\bar{\beta})}$ corresponds to the vector pointing from the $\bar{\beta}$ site of the tagged molecule to the α site on the ith atom/molecule. $\bar{x} = x^{(i\alpha,0\bar{\beta})}$, $\bar{y} = y^{(i\alpha,0\bar{\beta})}$ and $\bar{z} = z^{(i\alpha,0\bar{\beta})}$ correspond to the x, y, and z coordinates of this vector, and $\bar{r} = |\bar{\mathbf{r}}|$ corresponds to its length.

8. $\boldsymbol{u} = \boldsymbol{u}^{(\mathbf{0}\beta)}$ is the unit vector pointing from the center of of mass of the molecule to its β site. u_x, u_y and u_z are its x, y, and z components, respectively.

9. $w(r) \equiv r^3\phi'''(r) - 3r^2\phi''(r) + 3r\phi'(r)$, $v(r) \equiv r^2\phi''(r) - r\phi'(r)$ and $l(r) \equiv r\phi'(r)$, where $\phi'(r)$, $\phi''(r)$, and $\phi'''(r)$ are the first, second, and third derivatives of the LJ pair potential, $\phi(r)$, respectively.

With the above notations and conventions, one may write the overall potential energy in the following way:

$$V = \sum_{i=0}^{N_{act}-1} \sum_{j=i+1}^{N_t-1} \sum_{\alpha=1}^{n_s(i)} \sum_{\beta=1}^{n_s(j)} \phi(|\mathbf{r}^{(i\alpha)} - \mathbf{r}^{(j\beta)}|) + \sum_{i=0}^{N_{act}-1} \frac{1}{2}\delta(n_s(i), 2)\mu\omega^2(r^{(i\alpha,i\bar{\alpha})} - r_e)^2 \quad \text{(A1)}$$

It should also be noted that the potential energy includes the intramolecular vibrational energy of the molecules in the active cluster. The rigidity constraint imposed on those molecules is reintroduced at a later stage by discarding the corresponding high-frequency normal modes.

The LHA requires the calculation of the first and second derivatives of this potential energy with respect to the Cartesian coordinates of the atoms in the activated cluster.[66] Those are given by

$$\frac{\partial V}{\partial x^{(i\alpha)}} = \sum_{j\neq i}^{N_t} \sum_{\beta=1}^{n_s(j)} \phi'(r^{(i\alpha,j\beta)}) \frac{x^{(i\alpha,j\beta)}}{r^{(i\alpha,j\beta)}} + \delta(n_s(i), 2)\mu\omega^2(r^{(i\alpha,i\bar{\alpha})} - r_e)\frac{x^{(i\alpha,i\bar{\alpha})}}{r^{(i\alpha,i\bar{\alpha})}} \quad \text{(A2)}$$

$$\frac{\partial^2 V}{\partial x^{(i\alpha)}\partial x'^{(i'\alpha')}} = \sum_{j\neq i}^{N_t} \sum_{\beta=1}^{n_s(j)} \delta(\alpha,\alpha')\left[v(r^{(i\alpha,j\beta)})\frac{x^{(i\alpha,j\beta)}x'^{(i\alpha,j\beta)}}{(r^{(i\alpha,j\beta)})^4} + \delta(x, x')\frac{\phi'(r^{(i\alpha,j\beta)})}{r^{(i\alpha,j\beta)}}\right] + \delta(n_s(i), 2)\mu\omega^2\frac{x^{(i\alpha,i\bar{\alpha})}x'^{(i\alpha',i\bar{\alpha}')}}{r^{(i\alpha,i\bar{\alpha})}\, r^{(i\alpha,i\bar{\alpha})}} \text{ if } i' = i \quad \text{(A3)}$$

$$\frac{\partial^2 V}{\partial x^{(i\alpha)}\partial x'^{(i'\alpha')}} = -\, v(r^{(i\alpha,j\beta)})\frac{x^{(i\alpha,j\beta)}x'^{(i\alpha,j\beta)}}{(r^{(i\alpha,j\beta)})^4} - \delta(x, x')\frac{\phi'(r^{(i\alpha,j\beta)})}{r^{(i\alpha,j\beta)}}, \text{ if } i' \neq i \quad \text{(A4)}$$

Here, (x, x') correspond to any combination of x, y, and z, and $\delta(a, b)$ is the Kronecker δ function.

We next consider the calculation of the quantum nonlocal term $D_U(\mathbf{Q_0},\boldsymbol{P_{n,0}})$. The explicit expression of this term is given in ref 67. As shown there, calculating $D_U(\mathbf{Q_0},\boldsymbol{P_{n,0}})$ requires knowledge of the first and second derivatives of the potential force with respect to the atomic coordinates. Explicit expression of those derivatives are given below.

The first derivative of F_u with respect to the x coordinate of the atom at the β site of the tagged molecule is given by

$$\frac{\partial F_U}{\partial x^{(0\beta)}} = \frac{1}{2}\sum_{i=1}^{N_t-1} \sum_{\alpha=1}^{n_s(i)} \left[\phi''(r)\frac{x}{r^2}\mathbf{r}\cdot\mathbf{u} + \phi'(r)\left(-\frac{u_x}{r} + \frac{x}{r^3}\mathbf{r}\cdot\mathbf{u} + \frac{x}{rr_e}\right) - \phi'(\bar{r})\frac{\bar{x}}{\bar{r}r_e}\right] \quad \text{(A5)}$$

The first derivative of F_u with respect to the x coordinate of the atom at the α site of the other atoms or molecules is given by

$$\frac{\partial F_U}{\partial x^{(i\alpha)}} = \frac{1}{2}\sum_{\beta=1}^{2}\left[\phi''(r)\frac{x}{r^2}\mathbf{r}\cdot\mathbf{u} - \phi'(r)\left(-\frac{u_x}{r} + \frac{x}{r^3}\mathbf{r}\cdot\mathbf{u}\right)\right] \text{ if } i \neq 0 \quad \text{(A6)}$$

Similar expressions can be obtained for the corresponding derivatives with respect to the y and z coordinates, by replacing x with y or z.

The second derivative of F_u with respect to the x coordinate of the atom at the β site of the tagged molecule is given by

$$\frac{\partial^2 F_U}{\partial (x^{(0\beta)})^2} = \sum_{i=1}^{N_r-1}\sum_{\alpha=1}^{n_s(i)}\left\{\frac{w(r)x^2 + v(r)r^2}{2r^6}\mathbf{r}\cdot\mathbf{u} + v(r)\frac{xu_x}{r^4} - \frac{v(r)x^2 + l(r)r^2}{r^4 r_e}\right\} \quad \text{(A7)}$$

The second derivative of F_u with respect to the x and y coordinate of the atom at the β site of the tagged molecule is given by

$$\frac{\partial^2 F_U}{\partial x^{(0\beta)}\partial y^{(0\beta)}} = \sum_{i=1}^{N_r-1}\sum_{\alpha=1}^{n_s(i)}\left\{\frac{w(r)xy}{2r^6}\mathbf{r}\cdot\mathbf{u} + v(r)\frac{xu_y + yu_x}{2r^4} - \frac{v(r)xy}{r^4 r_e}\right\} \quad \text{(A8)}$$

The second derivative of F_u with respect to the x coordinate of the atom at the β site and the x coordinate of the atom at the other, $\bar{\beta}$, site of the tagged molecule is given by

$$\frac{\partial^2 F_U}{\partial x^{(0\beta)}\partial x^{(0\bar{\beta})}} = \sum_{i=1}^{N_r-1}\sum_{\alpha=1}^{n_s(i)}\left\{\frac{v(r)x^2 + l\,(r)r^2}{2r^4 r_e} + \frac{v(\bar{r})\bar{x}^2 + l\,(\bar{r})\bar{r}^2}{2\bar{r}^4 r_e}\right\} \quad \text{(A9)}$$

The second derivative of F_u with respect to the x coordinate of the atom at the β site and the y coordinate of the atom at the $\bar{\beta}$ site of the same tagged molecule is given by

$$\frac{\partial^2 F_U}{\partial x^{(0\beta)}\partial y^{(0\bar{\beta})}} = \sum_{i=1}^{N_r-1}\sum_{\alpha=1}^{n_s(i)}\left\{\frac{v(r)xy}{2r^4 r_e} + \frac{v(\bar{r})\bar{x}\,\bar{y}}{2\bar{r}^4 r_e}\right\} \quad \text{(A10)}$$

Similar expressions can be obtained for the other second derivatives with respect to the coordinates of the tagged molecule, by substituting the corresponding x, y, and z coordinates.

The second derivative of F_u with respect to the x coordinate of the atom at the β site of the tagged molecule and the x coordinate of the atom at the α site of the other atoms or molecules is given by

$$\frac{\partial^2 F_U}{\partial x^{(i\alpha)}\partial x^{(0\beta)}} = -\frac{1}{2}\left\{\frac{w(r)x^2 + v(r)r^2}{r^6}\mathbf{r}\cdot\mathbf{u} + 2v(r)\frac{xu_x}{r^4} - \frac{v(r)x^2 + l\,(r)r^2}{r^4 r_e} + \frac{v(\bar{r})\bar{x}^2 + l\,(\bar{r})\bar{r}^2}{\bar{r}^4 r_e}\right\} \quad \text{(A11)}$$

The second derivative of F_u with respect to the y coordinate of the atom at the β site of the tagged molecule and the x coordinate of the atom at the α site of the other atoms or molecules is given by

$$\frac{\partial^2 F_U}{\partial x^{(i\alpha)}\partial y^{(0\beta)}} = -\frac{1}{2}\left\{\frac{w(r)xy}{r^6}\mathbf{r}\cdot\mathbf{u} + v(r)\frac{xu_y + yu_x}{r^4} - \frac{v(r)xy}{r^4 r_e} + \frac{v(\bar{r})\bar{x}\,\bar{y}}{\bar{r}^4 r_e}\right\} \quad \text{(A12)}$$

Similar expressions can be obtained for the other second derivatives that mix the coordinates of the tagged molecule with those of the other atoms and molecules, by substituting the corresponding x, y, and z coordinates.

Finally, the second derivatives of F_u where both coordinates do not belong to the tagged molecule are given by

$$\frac{\partial^2 F_U}{\partial x^{(i\alpha)}\partial x^{(i\alpha)}} = \sum_{\beta=1}^{2}\left[\frac{w(r)x^2 + v(r)r^2}{2r^6}\mathbf{r}\cdot\mathbf{u} + v(r)\frac{xu_x}{r^4}\right] \quad \text{(A13)}$$

and

$$\frac{\partial^2 F_U}{\partial x^{(i\alpha)}\partial y^{(i\alpha)}} = \sum_{\beta=1}^{2}\left[\frac{w(r)xy}{2r^6}\mathbf{r}\cdot\mathbf{u} + v(r)\frac{xu_y + yu_x}{2r^4}\right] \quad \text{(A14)}$$

Here too, similar expressions can be obtained for the other second derivatives by substituting the corresponding x, y, and z coordinates.

References and Notes

(1) Brueck, S. R. J.; Osgood, R. M. *Chem. Phys. Lett.* **1976**, *39*, 568.
(2) Chateau, M.; Delalande, C.; Frey, R.; Gale, G. M.; Pradère, F. *J. Chem. Phys.* **1979**, *71*, 4799.
(3) Delalande, C.; Gale, G. M. *J. Chem. Phys.* **1979**, *71*, 4804.
(4) Delalande, C.; Gale, G. M. *J. Chem. Phys.* **1980**, *73*, 1918.
(5) Faltermeier, B.; Protz, R.; Maier, M.; Werner, E. *Chem. Phys. Lett.* **1980**, *74*, 425.
(6) Faltermeier, B.; Protz, R.; Maier, M. *Chem. Phys.* **1981**, *62*, 377.
(7) Oxtoby, D. W. *Adv. Chem. Phys.* **1981**, *47 (Part 2)*, 487.
(8) Oxtoby, D. W. *Annu. Rev. Phys. Chem.* **1981**, *32*, 77.
(9) Oxtoby, D. W. *J. Phys. Chem.* **1983**, *87*, 3028.
(10) Chesnoy, J.; Gale, G. M. *Ann. Phys. Fr.* **1984**, *9*, 893.
(11) Chesnoy, J.; Gale, G. M. *Adv. Chem. Phys.* **1988**, *70 (Part 2)*, 297.
(12) Harris, C. B.; Smith, D. E.; Russell, D. J. *Chem. Rev.* **1990**, *90*, 481.
(13) Miller, D. W.; Adelman, S. A. *Int. Rev. Phys. Chem.* **1994**, *13*, 359.
(14) Stratt, R. M.; Maroncelli, M. *J. Phys. Chem.* **1996**, *100*, 12981.
(15) Owrutsky, J. C.; Raftery, D.; Hochstrasser, R. M. *Annu. Rev. Phys. Chem.* **1994**, *45*, 519.
(16) Elsaesser, T.; Kaiser, W. *Annu. Rev. Phys. Chem.* **1991**, *42*, 83.
(17) Calaway, W. F.; Ewing, G. E. *J. Chem. Phys.* **1975**, *63*, 2842.
(18) Laubereau, A.; Kaiser, W. *Rev. Mod. Phys.* **1978**, *50*, 607.
(19) Roussignol, P.; Delalande, C.; Gale, G. M. *Chem. Phys.* **1982**, *70*, 319.
(20) Heilweil, E. J.; Doany, F. E.; Moore, R.; Hochstrasser, R. M. *J. Chem. Phys.* **1982**, *76*, 5632.
(21) Heilweil, E. J.; Casassa, M. P.; Cavanagh, R. R.; Stephenson, J. C. *Chem. Phys. Lett.* **1985**, *117*, 185.
(22) Heilweil, E. J.; Casassa, M. P.; Cavanagh, R. R.; Stephenson, J. C. *J. Chem. Phys.* **1986**, *85*, 5004.
(23) Harris, A. L.; Brown, J. K.; Harris, C. B. *Annu. Rev. Phys. Chem.* **1988**, *39*, 341.
(24) Paige, M. E.; Russell, D. J.; Harris, C. B. *J. Chem. Phys.* **1986**, *85*, 3699.
(25) Owrutsky, J. C.; Kim, Y. R.; Li, M.; Sarisky, M. J.; Hochstrasser, R. M. *Chem. Phys. Lett.* **1991**, *184*, 368.
(26) Moustakas, A.; Weitz, E. *J. Chem. Phys.* **1993**, *98*, 6947.
(27) Kliner, D. A. V.; Alfano, J. C.; Barbara, P. F. *J. Chem. Phys.* **1993**, *98*, 5375.
(28) Zimdars, D.; Tokmakoff, A.; Chen, S.; Greenfield, S. R.; Fayer, M. D. *Phys. Rev. Lett.* **1993**, *70*, 2718.
(29) Pugliano, N.; Szarka, A. Z.; Gnanakaran, S.; Hochstrasser, R. M. *J. Chem. Phys.* **1995**, *103*, 6498.
(30) Paige, M. E.; Harris, C. B. *Chem. Phys.* **1990**, *149*, 37.
(31) Salloum, A.; Dubost, H. *Chem. Phys.* **1994**, *189*, 179.
(32) Tokmakoff, A.; Sauter, B.; Fayer, M. D. *J. Chem. Phys.* **1994**, *100*, 9035.
(33) Tokmakoff, A.; Fayer, M. D. *J. Chem. Phys.* **1995**, *103*, 2810.
(34) Urdahl, R. S.; Myers, D. J.; Rector, K. D.; Davis, P. H.; Cherayil, B. J.; Fayer, M. D. *J. Chem. Phys.* **1997**, *107*, 3747.
(35) Owrutsky, J. C.; Li, M.; Locke, B.; Hochstrasser, R. M. *J. Phys. Chem.* **1995**, *99*, 4842.
(36) Laenen, R.; Rauscher, C.; Laubereau, A. *Phys. Rev. Lett.* **1998**, *80*, 2622.
(37) Woutersen, S.; Emmerichs, U.; Nienhuys, H.; Bakker, H. J. *Phys. Rev. Lett.* **1998**, *81*, 1106.

(38) Myers, D. J.; Urdahl, R. S.; Cherayil, B. J.; Fayer, M. D. *J. Chem. Phys.* **1997**, *107*, 9741.
(39) Myers, D. J.; Chen, S.; Shigeiwa, M.; Cherayil, B. J.; Fayer, M. D. *J. Chem. Phys.* **1998**, *109*, 5971.
(40) Sagnella, D. E.; Straub, J. E.; Jackson, T. A.; Lim, M.; Anfinrud, P. A. *Proc. Natl. Acad. Sci. U.S.A.* **1999**, *96*, 14324.
(41) Hamm, P.; Lim, M.; Hochstrasser, R. M. *J. Chem. Phys.* **1997**, *107*, 1523.
(42) Lawrence, C. P.; Skinner, J. L. *J. Chem. Phys.* **2002**, *117*, 5827.
(43) Deng, Y.; Stratt, R. M. *J. Chem. Phys.* **2002**, *117*, 1735.
(44) Deng, Y.; Stratt, R. M. *J. Chem. Phys.* **2002**, *117*, 10752.
(45) Sibert, E. L., III; Rey, R. *J. Chem. Phys.* **2002**, *116*, 237.
(46) Li, S.; Thompson, W. H. *J. Chem. Phys.* **2003**, *107*, 8696.
(47) Zwanzig, R. *J. Chem. Phys.* **1961**, *34*, 1931.
(48) Landau, L.; Teller, E. Z. *Z. Sowjetunion* **1936**, *34*, 10.
(49) Makri, N. *Annu. Rev. Phys. Chem.* **1999**, *50*, 167.
(50) Berne, B. J.; Jortner, J.; Gordon, R. *J. Chem. Phys.* **1967**, *47*, 1600.
(51) Bader, J. S.; Berne, B. J. *J. Chem. Phys.* **1994**, *100*, 8359.
(52) Egorov, S. A.; Everitt, K. F.; Skinner, J. L. *J. Phys. Chem. A* **1999**, *103*, 9494.
(53) Egorov, S. A.; Skinner, J. L. *J. Chem. Phys.* **2000**, *112*, 275.
(54) Skinner, J. L.; Park, K. *J. Phys. Chem. B* **2001**, *105*, 6716.
(55) Rostkier-Edelstein, D.; Graf, P.; Nitzan, A. *J. Chem. Phys.* **1997**, *107*, 10470.
(56) Rostkier-Edelstein, D.; Graf, P.; Nitzan, A. *J. Chem. Phys.* **1998**, *108*, 9598.
(57) Everitt, K. F.; Skinner, J. L.; Ladanyi, B. M. *J. Chem. Phys.* **2002**, *116*, 179.
(58) Berens, P. H.; White, S. R.; Wilson, K. R. *J. Chem. Phys.* **1981**, *75*, 515.
(59) Frommhold, L. Collision-induced absorption in gases. Vol. 2 of *Cambridge Monographs on Atomic, Molecular, and Chemical Physics*, 1st ed.; Cambridge University Press: Canbridge, England, 1993.
(60) Skinner, J. L. *J. Chem. Phys.* **1997**, *107*, 8717.
(61) An, S. C.; Montrose, C. J.; Litovitz, T. A. *J. Chem. Phys.* **1976**, *64*, 3717.
(62) Egorov, S. A.; Skinner, J. L. *Chem. Phys. Lett.* **1998**, *293*, 439.
(63) Schofield, P. *Phys. Rev. Lett.* **1960**, *4*, 239.
(64) Egelstaff, P. A. *Adv. Phys.* **1962**, *11*, 203.
(65) Kneller, G. R. *Mol. Phys.* **1994**, *83*, 63.
(66) Shi, Q.; Geva, E. *J. Phys. Chem. A* **2003**, *107*, 9059.
(67) Shi, Q.; Geva, E. *J. Phys. Chem. A* **2003**, *107*, 9070.
(68) Shi, Q.; Geva, E. *J. Chem. Phys.* **2003**, *118*, 8173.
(69) Sun, X.; Miller, W. H. *J. Chem. Phys.* **1997**, *106*, 916.
(70) Wang, H.; Sun, X.; Miller, W. H. *J. Chem. Phys.* **1998**, *108*, 9726.
(71) Sun, X.; Wang, H.; Miller, W. H. *J. Chem. Phys.* **1998**, *109*, 4190.
(72) Sun, X.; Wang, H.; Miller, W. H. *J. Chem. Phys.* **1998**, *109*, 7064.
(73) Wang, H.; Song, X.; Chandler, D.; Miller, W. H. *J. Chem. Phys.* **1999**, *110*, 4828.
(74) Sun, X.; Miller, W. H. *J. Chem. Phys.* **1999**, *110*, 6635.
(75) Wang, H.; Thoss, M.; Miller, W. H. *J. Chem. Phys.* **2000**, *112*, 47.
(76) Shemetulskis, N. E.; Loring, R. F. *J. Chem. Phys.* **1992**, *97*, 1217.
(77) Hillery, M.; O'Connell, R. F.; Scully, M. O.; Wigner, E. P. *Phys. Rep.* **1984**, *106* (3), 121.
(78) Everitt, K. F.; Skinner, J. L. *J. Chem. Phys.* **1999**, *110*, 4467.
(79) Whitnell, R. M.; Wilson, K. R.; Hynes, J. T. *J. Phys. Chem.* **1990**, *94*, 8625.
(80) Gai, H.; Voth, G. A. *J. Chem. Phys.* **1993**, *99*, 740.
(81) Gnanakaran, S.; Hochstrasser, R. M. *J. Chem. Phys.* **1996**, *105*, 3486.
(82) Berne, B. J.; Gordon, R. G.; Sears, V. F. *J. Chem. Phys.* **1968**, *49*, 475.
(83) Rey, R.; Hynes, J. T. *J. Chem. Phys.* **1996**, *104*, 2356.
(84) Perng, B.; Sasaki, S.; Ladanyi, B. M.; Everitt, K. F.; Skinner, J. L. *Chem. Phys. Lett.* **2001**, *348*, 491.
(85) Shi, Q.; Geva, E. *J. Chem. Phys.* **2003**, *118*, 7562.
(86) Jang, S.; Voth, G. A. *J. Chem. Phys.* **1997**, *107*, 9514.
(87) Press, W. H.; Flannery, B. P.; Teukolsky, S. A.; Vetterling, W. T. *Numerical Recipes*; Cambridge University Press: Cambridge, England, 1986.
(88) Nitzan, A.; Mukamel, S.; Jortner, J. *J. Chem. Phys.* **1974**, *60*, 3929.
(89) Nitzan, A.; Mukamel, S.; Jortner, J. *J. Chem. Phys.* **1975**, *63*, 200.
(90) Jacobsen, R. T.; Stewart, R. B.; Jahangiri, M. *J. Phys. Chem. Ref. Data* **1986**, *15*, 735.
(91) Sychev, V. V.; Vasserman, A. A.; Kozlov, A. D.; Spiridonov, G. A.; Tsymarny, V. A. *Thermodynamic Properties of Oxygen*, number 5 in National Standard Reference Data Service of the USSR: A Series of Property Tables; Hemisphere: Moscow, English ed., 1987.